Communications in Transportation Research 4 (2024) 100154

Contents lists available at ScienceDirect

Communications in Transportation Research

journal homepage: www.journals.elsevier.com/communications-in-transportation-research

Full Length Article

Traffic oscillation mitigation with physics-enhanced residual learning (PERL)-based predictive control

Keke Long, Zhaohui Liang, Haotian Shi, Lei Shi, Sikai Chen **, Xiaopeng Li *

Department of Civil and Environmental Engineering, University of Wisconsin–Madison, Madison, WI, 53706, USA

ARTICLE INFO

Keywords:
Traffic oscillations
Traffic safety
Connected and autonomous vehicle
Mix traffic
Vehicle-in-the-loop

ABSTRACT

Real-time vehicle prediction is crucial in autonomous driving technology, as it allows adjustments to be made in advance to the driver or the vehicle, enabling them to take smoother driving actions to avoid potential collisions. This study proposes a physics-enhanced residual learning (PERL)-based predictive control method to mitigate traffic oscillation in the mixed traffic environment of connected and automated vehicles (CAVs) and human-driven vehicles (HDVs). The introduced model includes a prediction model and a CAV controller. The prediction model is responsible for forecasting the future behavior of the preceding vehicle on the basis of the behavior of preceding vehicles. This PERL model combines physical information (i.e., traffic wave properties) with data-driven features extracted from deep learning techniques, thereby precisely predicting the behavior of the preceding vehicle, especially speed fluctuations, to allow sufficient time for the vehicle/driver to respond to these speed fluctuations. For the CAV controller, we employ a model predictive control (MPC) model that considers the dynamics of the CAV and its following vehicles, improving safety and comfort for the entire platoon. The proposed model is applied to an autonomous driving vehicle through vehicle-in-the-loop (ViL) and compared with real driving data and three benchmark models. The experimental results validate the proposed method in terms of damping traffic oscillation and enhancing the safety and fuel efficiency of the CAV and the following vehicles in mixed traffic in the presence of uncertain human-driven vehicle dynamics and actuator lag.

1. Introduction

Traffic oscillations, commonly referred to as ‘stop-and-go’ traffic, epitomize the fluctuation between slow-moving and fast-moving states in congested traffic, deviating from a steady flow (Li et al., 2010, 2014). This widespread phenomenon in human driving scenarios presents several critical issues. First, it exacerbates the risk of accidents by complicating the maintenance of safe vehicle distances, thus increasing collision probabilities (Li et al., 2012; Yao et al., 2020). Second, it diminishes traffic efficiency, inducing congestion and a ripple effect that disrupts numerous vehicles. Moreover, the frequent acceleration and deceleration cycles escalate fuel consumption and emissions (Stern et al., 2019), detrimentally impacting the environment.

The evolution of connected and automated vehicle (CAV) technologies offers a promising solution to mitigate traffic oscillations (Ghiasi et al., 2019; He et al., 2024; Larsson et al., 2021; Wang et al., 2023). CAVs leverage advanced perception systems and trajectory planning. In the perception part, CAVs can perceive information about preceding vehicles, anticipating the traffic oscillations ahead (Zhou et al., 2017). In a connected scenario, lead vehicles harness vehicle-to-everything (V2X) technology to collect and analyze traffic data. Conversely, in non-connected settings, roadside units and monitoring systems can gather traffic information for real-time predictions and advisories and send the information to the target vehicle through dynamic message signs. This gathered data enables the identification of traffic oscillation patterns, facilitating accurate predictions and allowing the vehicle to determine when it might be impacted (Yao et al., 2023). Downstream oscillation patterns not only facilitate accurate predictions but also inform the strategic planning and control phases of CAV operation (Fang et al., 2024). Researchers have captured the formation and ensuing propagation of stop-and-go waves and predicted traffic oscillation via the behavioral car-following model (Chen et al., 2012) and neural network-based models (Zhou et al., 2017). By understanding the likely traffic conditions in advance, CAVs can optimize their trajectory planning to either avoid or mitigate potential impacts from identified oscillations. This proactive integration of prediction and planning enables a more

* Corresponding author.
** Corresponding author.
E-mail addresses: sikai.chen@wisc.edu (S. Chen), xli2485@wisc.edu (X. Li).

https://doi.org/10.1016/j.commtr.2024.100154
Received 4 July 2024; Received in revised form 2 August 2024; Accepted 7 August 2024
Available online 28 November 2024

coherent approach to traffic management, ensuring that CAVs dynamically adjust their behavior to maintain optimal flow and enhance overall traffic safety.

For perception, most existing CAV controllers mitigate traffic oscillation on the basis of the predicted behavior of the preceding vehicle (Hu et al., 2021; Wang et al., 2023) or aggregated information, e.g., average vehicle speed (Stern et al., 2019). Relying solely on the predicted behavior of the preceding vehicle is insufficient for predictive safety measures. This may raise two main issues. First, traffic oscillation originates downstream (Zheng et al., 2022). The wave fluctuations upstream are difficult to perceive if only one preceding vehicle is considered. Second, when fluctuations in the preceding vehicle are detected, it is usually too late for the following CAV to respond appropriately, with consideration of the communication delay and actuator lag. Therefore, to predict the state of preceding vehicles effectively, information from multiple vehicles in front is required as input.

In the realm of predicting downstream multivehicle trajectories, most studies have adopted physics-based models to model and predict vehicle trajectories. In this research, the "physics model" or "physics rules" refer to theoretical or empirical formulations that describe the behavior of physical systems. These models are often based on fundamental principles such as conservation laws, equations of motion, or thermodynamics, which are structured to explain and predict the dynamics of systems under various conditions. In the context of shockwave modeling. The physics of shockwaves is a fundamental traffic flow characteristic that was first studied by the Lighthill–WhithamRichards (LWR) model (Lighthill and Whitham, 1997). Shockwaves in congested traffic usually follow "stop-and-go" patterns that could cause adverse consequences. These models typically utilize the historical data of the subject vehicle and its immediate predecessor to predict future trajectories for a limited number of time steps, which may not suffice for the CAV controller. Moreover, physics models may struggle to capture the complex interactions and nonlinear behaviors prevalent in dense traffic conditions (Durrani et al., 2016; Punzo and Montanino, 2020). Recently, researchers have turned to data-driven methods because of their ability to detect intricate patterns and adapt to diverse datasets (Yao et al., 2022). However, these learning-based methods often require substantial training data (Karniadakis et al., 2021; Li et al., 2022) and lack interpretability. In response to these challenges, the physics-informed neural network (PINN) method has been utilized to increase the applicability of Neural Network (NN) models in scenarios with limited data samples (Mo et al., 2021; She and Ouyang, 2024). This is achieved by incorporating physical models to augment data and regularizing the models to prevent overfitting, although this method is contingent on the accuracy of the physical models and can lead to unstable training processes (Yao et al., 2023).

Recognizing the complementary strengths and weaknesses of these methodologies, the physics-enhanced residual learning (PERL) framework was proposed to combine the robust interpretability of physics models with the adaptive precision of learning-based models (Long et al., 2024a). By focusing on the physics model residuals—the differences between the predictions of the physics model and observed data—PERL leverages a neural network to refine these predictions. This method enhances the accuracy of trajectory forecasts, maintains the model's interpretability, and reduces its dependency on extensive datasets. Consequently, PERL stands out for its ability to deliver high-precision and stable predictions of future vehicle behaviors, offering a balanced synthesis of the theoretical and empirical realms. When applied to downstream multivehicle scenarios, the PERL method effectively extracts the characteristics of downstream oscillation propagation, significantly improving the long-term predictive performance for preceding vehicles. This methodology offers a balanced synthesis of theoretical and empirical insights, ensuring high-precision and stable predictions of future vehicle behaviors.

On the basis of the predictions of preceding vehicles with traffic oscillation, the CAV controller can mitigate oscillation amplification and backward propagation, thus enhancing overall traffic stability. Moreover, it is crucial to account for the behavior of the following vehicles (Gao et al., 2022). Considering the actions of these following vehicles, particularly in mixed traffic scenarios, designing safer and more efficient trajectories is essential (Mohammadian et al., 2023). This anticipation helps minimize the occurrence of sudden driving maneuvers, thereby enhancing the overall safety and fluidity of traffic. Given that traffic will likely comprise a mix of autonomous and human-driven vehicles for foreseeable means, this presents distinct challenges and opportunities for trajectory optimization. Compared with CAVs, human-driven vehicles (HVs) tend to display less predictable behavior. This unpredictability increases the complexity of trajectory planning for CAVs, requiring more sophisticated prediction algorithms and adaptive control strategies, particularly when a CAV is followed by an HV.

Reflecting on the identified research gaps, this study aims to introduce a physics-enhanced CAV controller. Our approach involves developing control strategies specifically tailored for mixed platoons comprising both CAVs and HVs on the basis of predicted information of the downstream traffic from the PERL model. In particular, we focus on scenarios where a CAV is followed by an HV, effectively addressing the dynamics of mixed traffic flows. This strategy incorporates the formulation of a model predictive control (MPC) system that considers the formation of both CAVs and HVs within the control objectives (Chen et al., 2018). While direct control is exerted only over the CAVs, the states of the HVs are also integrated into the optimization objectives, ensuring that the overall strategy accounts for the behavioral patterns of both autonomous and human drivers. By employing the advanced predictive PERL model and adaptive control strategy, our MPC framework optimizes traffic behavior across different vehicle types, considering the interactive dynamics inherent in mixed vehicle streams.

The primary contributions of this work are threefold. First, a PERL-based trajectory prediction method is designed to extract the characteristics of downstream oscillation propagation from the historical trajectories of multiple preceding vehicles. This method enables interpretable and highly accurate long-term trajectory predictions for preceding vehicles. Second, during the planning phase, this method considers the impact of oscillations from preceding vehicles, whereas the mixed platoon MPC controller also accounts for the influence of following vehicles. This comprehensive consideration enhances the management and performance of mixed platoons comprising both CAVs and HVs. Third, the performance of the proposed method is validated through real-vehicle experiments. Existing studies predominantly involve simulations (Bai et al., 2022; Li et al., 2017, 2021; Qu et al., 2020) or miniature experiments (Wang et al., 2024), which cannot fully address the complex challenges of real-world implementations, such as feedback delay, actuator lag, measurement inaccuracy, and the heterogeneity of traffic flows. These limitations highlight the essential need for experiments with actual vehicles. However, evaluating the effectiveness of the proposed control algorithms through real-vehicle experiments introduces significant technical challenges. The interaction of a controlled CAV with other vehicles in live traffic conditions poses safety risks. Moreover, equipping a fleet of test vehicles for such experiments is resource intensive. Thus, a vehicle-in-the-loop (ViL) methodology is employed to address these challenges (Xu et al., 2017). The experimental simulation involves a mixed traffic scenario involving six vehicles, with four preceding vehicles derived from the NGSIM I80 dataset. Using the proposed PERL-based predictive control, vehicle speed commands are generated and relayed to the test vehicle operating on the test track. Concurrently, the ViL system simulates the behavior of the following HV, providing a comprehensive test environment that bridges simulation and real-world conditions.

The rest of this paper is organized as follows. Section 2 presents the investigated problem. Section 3 proposes the PERL-based predictive control model. Section 4 conducts a ViL experiment to compare the proposed model with the existing traffic dataset benchmark. Section 5 concludes this study and discusses future research.

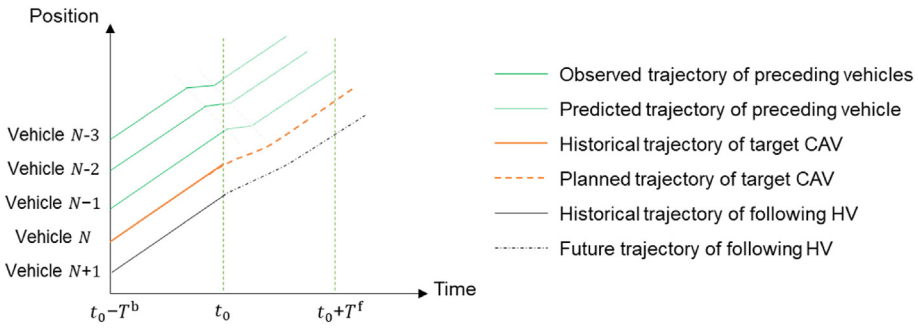

Fig. 1. CAV trajectory planning based on multiple preceding vehicle predictions.

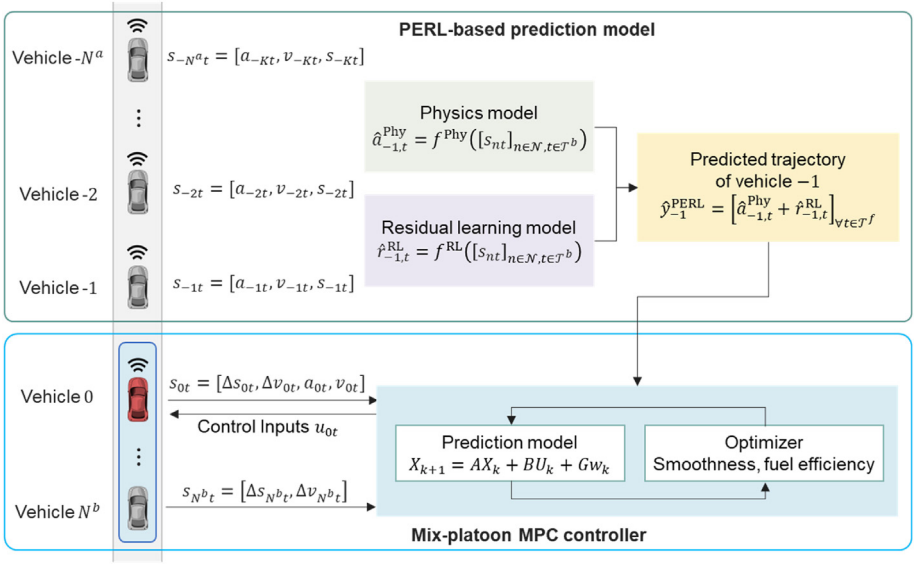

Fig. 2. PERL-based predictive control (PERL-MPC) model.

2. Problem statement

This study investigates a CAV controller using multistep real-time downstream vehicle trajectory data to assist roadway safety and dampen traffic oscillation in mixed traffic. As shown in Fig. 1, a stream of vehicles operates in a single-lane roadway segment. The subject CAV is indexed by N. The preceding vehicles (indexed by 1 to $N-1$ from downstream to upstream). At time t, the future longitudinal behavior of the preceding vehicles is predicted from t_0 to $t_0 + T^{\text{f}}$, on the basis of the historical trajectory from $t_0 - T^{\text{b}}$ to t_0, where T^{b} is the backward observation period and T^{b} is the forward prediction period. Time is discretized with a small interval δ in this study because vehicle trajectory data are discretized in time.

The model first predicts the future behavior of vehicle $N-1$, and then the planning model output is the future planned trajectory of vehicle N. The main objective here is to leverage the predictive capabilities of PERL to better anticipate the situational behavior of vehicles in its vicinity and plan the AV trajectory accordingly.

Note that this research is applicable to mixed traffic. The types of preceding vehicles and the following vehicles are not assumed since the heterogeneity of the vehicles is considered. We assume that the target vehicle could have the information of its preceding $N-1$ vehicles and the following vehicle. The heterogeneity is captured by their trajectory during the observation period.

The objective is to construct a control model for the target CAV to yield a trajectory on the basis of the prediction of the preceding vehicle. The detailed methodology is presented in Section 3.

3. Methodology

On the basis of the problem statement, this section presents the proposed PERL-based predictive control model that aims to mitigate traffic oscillation. As shown in Fig. 2, this model contains two main components: the PERL-based prediction model and the mixed platoon MPC controller. A mixed platoon of N^{b} vehicles is controlled by the MPC controller based on the information provided by preceding N^a vehicles.

3.1. PERL-based prediction model

This component is designed to forecast the future states of the preceding vehicle, incorporating physical laws and residual learning mechanisms to enhance prediction accuracy and stability. By integrating physical models with deep learning techniques, the PERL model effectively anticipates traffic oscillations, providing a robust foundation for downstream control decisions (Long et al., 2024a).

As shown in Fig. 2, an input state stems from a set of K consecutive vehicles upstream of the subject CAV, indexed by $k \in \mathcal{K} := \{-1, -2, \ldots, -K\}$ from the upstream lead vehicle indexed by

-1 through the upstream vehicle by $-K$, at T^{b} historical observation points, where $\mathscr{T}^{\mathrm{b}} := \{t_0 - (T^{\mathrm{b}} - 1)\delta, \ldots, t_0 - \delta, t_0\}$. The input state is defined as $s = [a_{nt}, v_{nt}, \Delta d_{nt}]_{\forall n \in \mathscr{N}, t \in \mathscr{T}^{\mathrm{b}}}$, where a_{kt}, v_{kt}, and Δd_{kt} are the acceleration, speed, and spacing (from the preceding vehicle) of vehicle k at time t in sample i, respectively. The prediction output is the trajectory of preceding vehicle -1 at future time points $\mathscr{T}^{\mathrm{f}} := \{t_0 + \delta, t_0 + 2\delta, \ldots, t_0 + T^{\mathrm{f}}\delta\}$, i.e., $\hat{y}_{-1}^{\mathrm{PERL}} = [\hat{a}_{-1t}]_{t \in \mathscr{T}^{\mathrm{f}}}$, where $\hat{a}_{-1t}$ is the predicted acceleration of vehicle -1 at a future time point t.

In the physics component, $S^{\mathrm{Phy}}(\cdot)$ projects s to a much lower-dimensional space, i.e., $S^{\mathrm{Phy}}(s) = [a_{kt_k}, v_{kt_k}, \Delta d_{kt_k}]_{k \in \mathscr{K}, t_k \in [t_0 - \tau_k, \ldots, t_0]}$ or its subset where τ_k is a short reaction time depending on the specific physics model $t_0 - \tau_k \in \mathscr{T}^{\mathrm{b}}$. With this, $|\Theta^{\mathrm{Phy}}|$ is on the order of $|S^{\mathrm{Phy}}(s)|$, i.e., $O(|S^{\mathrm{Phy}}(s)|)$, and thus much smaller than $|\mathscr{S}|$. $\mathscr{Y}^{\mathrm{Phy}}$ is the predicted acceleration of vehicle K: $[\hat{a}_{Kt}^{\mathrm{Phy}}(\theta^{\mathrm{Phy}})]_{\forall t \in \mathscr{T}^{\mathrm{f}}} = f^{\mathrm{Phy}}(S^{\mathrm{Phy}}(s)|\theta^{\mathrm{Phy}})$. Therefore, we obtain the residual acceleration predicted by the physics model $r_{Kt}(\theta^{\mathrm{Phy}}) := g(s) - \hat{a}_{Kt}^{\mathrm{Phy}}(\theta^{\mathrm{Phy}}), \forall t \in \mathscr{T}^{\mathrm{f}}$.

In the residual learning component, $|\Theta^{\mathrm{RL}}|$ is generally polynomial in relation to $|s|$ and the architecture of the model; thus, $|\Theta^{\mathrm{RL}}|$ is likely much greater than $|\Theta^{\mathrm{Phy}}|$. $\mathscr{Y}^{\mathrm{RL}}$ is the predicted residual of vehicle K: r_{Kt}, i.e., $[\hat{r}_{Kt}^{\mathrm{RL}}(\theta^{\mathrm{RL}})]_{\forall t \in \mathscr{T}^{\mathrm{f}}} = f^{\mathrm{RL}}(s|\theta^{\mathrm{RL}})$. Therefore, the output of the PERL model is $f^{\mathrm{PERL}}(s|\theta^{\mathrm{PERL}}) = [\hat{a}_{Kt}^{\mathrm{Phy}}(\theta^{\mathrm{Phy}}) + \hat{r}_{Kt}^{\mathrm{RL}}(\theta^{\mathrm{RL}})]_{\forall t \in \mathscr{T}^{\mathrm{f}}}$.

For the physics component, we employ a shockwave-based car-following model. This model uses shockwave dynamics to predict vehicle behavior on the basis of the movement of surrounding vehicles. The predicted future speeds are calculated on the basis of the relative positions and the defined wave speed. This model notably expands the scope of traditional car-following models by incorporating the effects of multiple vehicles in proximity, not just those directly ahead, providing a more comprehensive analysis of traffic dynamics.

For the residual learning component, we utilized a convolution long short-term memory (CLSTM) model to capture the dynamic and sequential nature of vehicle driving behaviors effectively. Integrating convolutional layers in the CLSTM model aims to abstract and understand the overall trends and variations within the input data (Yao et al., 2023). These convolutional layers are adept at handling spatial dependencies and mitigating the impact of minor inaccuracies in the data, which can be crucial for maintaining robustness in predictions. The LSTM component of the model aims to capture temporal dependencies and the sequence of events in the vehicle states over time, aligning with the fundamental car-following rule where vehicles follow each other in sequence from downstream to upstream. This sequence-sensitive processing allows the model to anticipate future vehicle behaviors on the basis of past and current observations, providing predictive insight that is more closely aligned with actual driving behaviors than traditional models are.

The proposed CLSTM model structure begins with an input layer that takes in the state of vehicles. These data pass through a convolutional layer where initial feature extraction occurs. The subsequent LSTM layers delve deeper into these features, analyzing the time-related dependencies and evolving conditions in the traffic environment. Dropout layers interspersed among the LSTM layers help prevent overfitting by randomly omitting subsets of features during training, which enhances the model's generalizability. This sequence concludes with dense layers that consolidate the learned features into outputs that predict vehicle behaviors, followed by a final dropout layer to further refine the output by minimizing overfitting. Therefore, the CLSTM architecture combines the strengths of convolutional neural networks in feature extraction and LSTM networks in sequence modeling, making it particularly suitable for complex, dynamic traffic scenarios.

3.2. Mix-platoon MPC model

Building on the predictions generated by the PERL model, the MPC component optimizes the trajectory of the controlled vehicle in real time. It considers the dynamic constraints of the traffic environment and the vehicle's operational limitations, aiming to minimize the impact of traffic oscillations on the controlled vehicle and, by extension, the surrounding traffic flow. The primary objective of the MPC model is to improve traffic efficiency and safety by adjusting the vehicle's speed and position in a predictive manner.

3.2.1. Single CAV dynamic model

We first introduce a longitudinal dynamics model for a single CAV. Its nonlinear longitudinal dynamic model can be described as

$$\begin{cases} \dfrac{\mathrm{d}s}{\mathrm{d}t} = v \\ \dfrac{\mathrm{d}v}{\mathrm{d}t} = a \\ \dfrac{\mathrm{d}a}{\mathrm{d}t} = f(v,a) + g(v)\eta \end{cases} \tag{1}$$

where s, v, and a are the position, velocity, and acceleration of the vehicle, respectively, and η is the engine input. Functions f and g are given by

$$f(v,a) = -\frac{2K_{\mathrm{d}}}{m}va - \frac{1}{\tau_n^A}\left[a + \frac{K_{\mathrm{d}}}{m}v^2 + \frac{d_{\mathrm{m}}}{m}\right] \tag{2}$$

$$g(v) = \frac{1}{m\tau_n^A} \tag{3}$$

where K_{d} represents the aerodynamic drag coefficient, m represents the vehicle mass, τ_n^A represents the engine time lag, and d_{m} represents the mechanical drag. In this study, we focus on the longitudinal kinematics of vehicles. Assuming that the parameters in Eqs. (4) and (5) are known a priori, we adopt the following control law structure to implement feedback linearization:

$$\eta = mu + K_{\mathrm{d}}v^2 + d_{\mathrm{m}} + 2\tau_n^A K_{\mathrm{d}}va \tag{4}$$

where u is the desired acceleration, which is determined by the upper controller.

By substituting Eqs. (2)–(4) into Eq. (1), the differential equation of acceleration can be rewritten as

$$\dot{a_n} = \frac{u_n - a_n}{\tau_n^A} \tag{5}$$

The objectives of CAV planning are to follow the preceding vehicle with the desired spacing distance and ensure safety. Therefore, a constant time headway (CTH) spacing strategy was applied. The desired spacing distance of vehicle n is $s_n^d = hv_n + d$, where h and d are the desired constant headway and space at a standstill, respectively. On the basis of the CTH rule, the position error Δs with respect to a desired distance from the preceding vehicle $\Delta s = s_{n-1} - s_n - l_{n-1} - s_n^d$ and l_{n-1} is the length of the preceding vehicle.

Given the system state $\boldsymbol{x} = [\Delta s, \Delta v, a]^{\mathrm{T}}$, Δv is the velocity error between the ego and the preceding vehicle: $\Delta v = v_{n-1} - v_n$. The control variable $\boldsymbol{u} = u_n$, where u_n is the desired acceleration, the outside disturbance is the acceleration of the preceding vehicle $\boldsymbol{d} = a_{n-1}$, and the longitudinal dynamics state-space model of the CAV is as Eq. (6):

$$\frac{\mathrm{d}}{\mathrm{d}t}\boldsymbol{x}=\frac{\mathrm{d}}{\mathrm{d}t}\begin{pmatrix}\Delta s\\ \Delta v\\ a\end{pmatrix}=\frac{\mathrm{d}}{\mathrm{d}t}\begin{pmatrix}s_{n-1}-s_n-l_n-s_n^d\\ v_{n-1}-v_n\\ a_n\end{pmatrix}=\begin{pmatrix}v_{n-1}-v_n-l_n-s_n^d\\ a_{n-1}-a_n\\ (u_n-a_n)/\tau_n^A\end{pmatrix}=\boldsymbol{Ax}+\boldsymbol{Bu}+\boldsymbol{Cd} \tag{6}$$

where

$$\boldsymbol{A}=\begin{bmatrix}0&1&-h\\0&0&-1\\0&0&-\frac{1}{\tau_n^A}\end{bmatrix},\boldsymbol{B}=\begin{bmatrix}0\\0\\\frac{1}{\tau_n^A}\end{bmatrix},\boldsymbol{C}=\begin{bmatrix}0\\1\\0\end{bmatrix} \tag{7}$$

3.2.2. Car-following behavior of HVs

In this study, we use the IDM as the CF model. The IDM is widely used and studied in the literature because it can successfully produce stop-and-go oscillations in congested traffic. The IDM model provides a model acceleration function as a continuous function of the velocity, gap, and velocity difference and is expressed as Eqs. (8) and (9):

$$\begin{cases}\dfrac{\mathrm{d}s}{\mathrm{d}t}=v\\ \dfrac{\mathrm{d}v}{\mathrm{d}t}=\overline{a}\left[1-\left(\dfrac{v_t^n}{v^f}\right)^4-\left(\dfrac{S^*\left(v_t^n,\Delta v_t^n\right)}{\Delta x_t^n}\right)^2\right]\end{cases} \tag{8}$$

$$S^*\left(v_t^n,\Delta v_t^n\right)=S_0+t_0v_t^n-\frac{v_t^n\cdot\Delta v_t^n}{2\sqrt{\overline{a}\overline{b}}} \tag{9}$$

where $\overline{a}$ is the maximum acceleration of the vehicle, $\overline{b}$ is the comfortable deceleration, and S_0 and t_0 are parameters representing the minimum desired distance to the car in front and the time headway, respectively. v^f is the desired speed.

3.2.3. Heterogeneous platoon dynamics model

Consider one CAV with several HVs driving following it; here, we consider the simplest situation, with only one HV following it, as shown in Fig. 3. For this platoon, the state and control variables can be defined as $\boldsymbol{x}^{\mathrm{H}}=(\Delta s_0,\Delta v_0,a_0,\Delta s_1,\Delta s_1)^{\mathrm{T}}$ and $\boldsymbol{u}^{\mathrm{H}}=(u_0)^{\mathrm{T}}$, and the exogeneous disturbance is $\boldsymbol{w}^{\mathrm{H}}=(a_{-1},a_1)$.

The longitudinal dynamics model for the platoon formed by a leading CAV and the following HV is as Eq. (10):

$$\frac{\mathrm{d}}{\mathrm{d}t}\boldsymbol{x}^{\mathrm{H}}=\frac{\mathrm{d}}{\mathrm{d}t}(\Delta s_0,\Delta v_0,a_0,\Delta s_1,\Delta v_1)^{\mathrm{T}}=\boldsymbol{A}^{\mathrm{H}}\boldsymbol{x}^{\mathrm{H}}+\boldsymbol{B}^{\mathrm{H}}\boldsymbol{u}^{\mathrm{H}}+\boldsymbol{C}^{\mathrm{H}}\boldsymbol{w}^{\mathrm{H}} \tag{10}$$

where

$$\boldsymbol{A}^{\mathrm{H}}=\begin{bmatrix}\boldsymbol{A}_{n=1}&0^{3\times2}\\0^{2\times2}&\boldsymbol{D}^{2\times3}\end{bmatrix},\boldsymbol{B}^{\mathrm{H}}=\begin{bmatrix}0\\0\\\frac{1}{\tau_n^A}\end{bmatrix},\boldsymbol{C}^{\mathrm{H}}=\begin{bmatrix}\boldsymbol{C}&0^{3\times1}\\0^{2\times1}&\boldsymbol{E}\end{bmatrix},\boldsymbol{D}^{2\times3}=\begin{bmatrix}0&0&1\\1&0&0\end{bmatrix},\boldsymbol{E}=\begin{bmatrix}-T\\-1\end{bmatrix} \tag{11}$$

3.2.4. Model predictive control (MPC) algorithm

Consider a linear discrete-time state-space model given in Eqs. (12) and (13):

$$x_{t+1}=Ax_t+B_1u_t+B_2w_t \tag{12}$$

$$y_{t+1}=Cx_t \tag{13}$$

where $x_{t+1}\in R^n$ is the system state; $y_{t+1}\in R^m$ is the measured output; $u_t\in R^p$ is the control input; and w_t is the disturbance input. We assume that the state and disturbance vectors can be measured in every sampling period. The designed controller regulates platoon desired accelerations over a time horizon $[t_0,t_0+N_{\mathrm{c}}]$ to minimize a cost function J representing driving safety, efficiency, and ride comfort. Considering that the strict constraints of MPC may make the optimization problem infeasible, a slack variable is introduced here to soften the constraints. We add the slack variable into the optimization problem:

$$\min_{\Delta\boldsymbol{u}[t_0,t_0+N_{\mathrm{c}}]}J=\sum_{j=0}^{N-1}\left\|\Delta s_{t+j|t}\right\|_Q^2+\sum_{j=0}^{N_{\mathrm{c}}-1}\left\|\Delta u_{k+j|k}\right\|_R^2+\boldsymbol{\varepsilon}^{\mathrm{T}}\rho\boldsymbol{\varepsilon} \tag{14}$$

where N is the predictive horizon length and where N_{c} is the control horizon length. Q and R are the weight matrices of the error and input, respectively. ε is the slack vector, and ρ is its weight. The optimization objective is subjected to the following constraints, where $\sigma_{\min}^y$ and $\sigma_{\max}^y$ are specific scaling factors applied to the constraints:

$$\Delta s_{\min}+\varepsilon\sigma_{\min}^y\le s_{t+j|t}\le\Delta s_{\max}+\varepsilon\sigma_{\max}^y \tag{15}$$

$$v_{\min}+\varepsilon\sigma_{\min}^y\le v_{t+j|t}\le v_{\max}+\varepsilon\sigma_{\max}^y \tag{16}$$

$$u_{\min}+\varepsilon\sigma_{\min}^u\le u_{t+j|t}\le u_{\max}+\varepsilon\sigma_{\max}^u \tag{17}$$

4. Experiments

4.1. Experiment settings

We conducted a series of experiments to validate the above-proposed methodology. For the experiment, this section introduces the setting of the ViL experiment, including the data preparation, the researched CAV, the ViL testing environment, and the baseline controllers.

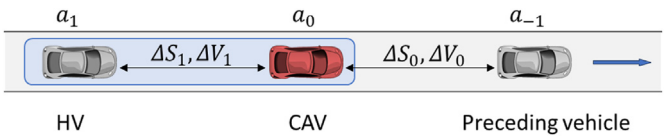

Fig. 3. Heterogeneous platooning of a CAV followed by an HV.

4.1.1. Data preparation

In the field experiment, the proposed PERL-based controller is validated via the widely applied next-generation simulation (NGSIM) dataset (NGSIM, 2007). The trajectory of 6 consecutive vehicles is extracted as the result of Baseline 1. For other baseline situations and the proposed situation, the preceding 4 vehicles of the 6 vehicles are used as the trajectory of Vehicle -1 to Vehicle $-K$, $K = 4$.

Six sample trips were chosen for the experiments, which included two sets from acceleration trips, two from deceleration trips, and two from cruising trips. These trips are labeled Trip 1 through Trip 5, each with a duration of 20 s. Considering the heterogeneity of the traffic flow, the headway h^d for each vehicle was calibrated on the basis of its trajectory (Long et al., 2024b).

4.1.2. ViL environment

This study employs a ViL approach with the experimental setup illustrated in Fig. 4 and the experimental parameters presented in Table 1. In this setting, our algorithm sets a maximum speed limit of 15 m/s to ensure safety, considering the constraints of the test track environment. The experimental environment comprises two parts: a simulation and a field experiment. Six vehicles are simulated in the simulation, where the trajectories of the first four vehicles are extracted from the total NGSIM dataset. The fifth vehicle is a controlled CAV, and the sixth vehicle is an HV. During the experiment, the trajectories of the preceding vehicles are transmitted to the physical CAV as inputs to the control model. The onboard computer subsequently applies PERL-based predictive control to derive the longitudinal target speed, which is relayed to the vehicle's lower-level actuation system. The vehicle's actual position on the test track is fed back into the simulation environment for updates.

In the field experiment segment, the physical CAV is the Lincoln MKZs 2016. The vehicle's lower-level control contains longitudinal and lateral dynamics, where the longitudinal behavior is governed by piecewise PID control, and an MPC controller manages the lateral behavior.

The field experiments are conducted at the test track in Madison, WI, USA. Fig. 4 shows a satellite image of the test track. We conduct experiments on an approximately 300 m straight road segment. There are two lanes on the road; each lane is 3.5 m in width, with shoulders on the boundary of the road segment. Moreover, the road segment is level without superelevation or grades. Fig. 5 shows the interior view of the experimental vehicle during the experiment. A safety operator is responsible for driving the vehicle to the starting point of the test track and then initiating a program that allows the vehicle's computer to control the vehicle. The safety operator does not operate the accelerator pedal or the steering wheel. In the case of emergency situations (e.g., unexpected obstacles), the safety operator will take over vehicle control to ensure safety. Another individual, the data collector, is responsible for operations related to data collection.

4.1.3. Baseline methods

To validate the effectiveness of the two components in our proposed method in mitigating traffic oscillation, we compared it with different model components. We set up three baseline methods compared with the proposed control method (Fig. 6):

Baseline 1: No prediction or control. All the vehicles are HVs without control. This baseline is extracted from the original NGSIM dataset.

Baseline 2: MPC applied to CAV with PERL-based prediction. The following HV is not considered in the MPC control model.

Baseline 3: MPC is applied to CAVs with CLSTM-based prediction by preceding vehicle information. The following HV is not considered in the MPC control model.

Proposed controller: MPC is applied to a mixed platoon of CAVs and HVs with PERL-based prediction. The first four vehicles are called preceding vehicles with a designed trajectory from the dataset; the fifth vehicle is a CAV, and the sixth vehicle is an HV. The physics model utilized the shockwave-based Newell car-following model, augmented with the terminal state connection process in Section 3.2. For the NN model, we choose a CLSTM model, which is the same as the NN component in the PINN model.

4.1.4. Measurements

To comprehensively evaluate the proposed method, our measurements encompass three aspects: safety, oscillation propagation, and fuel

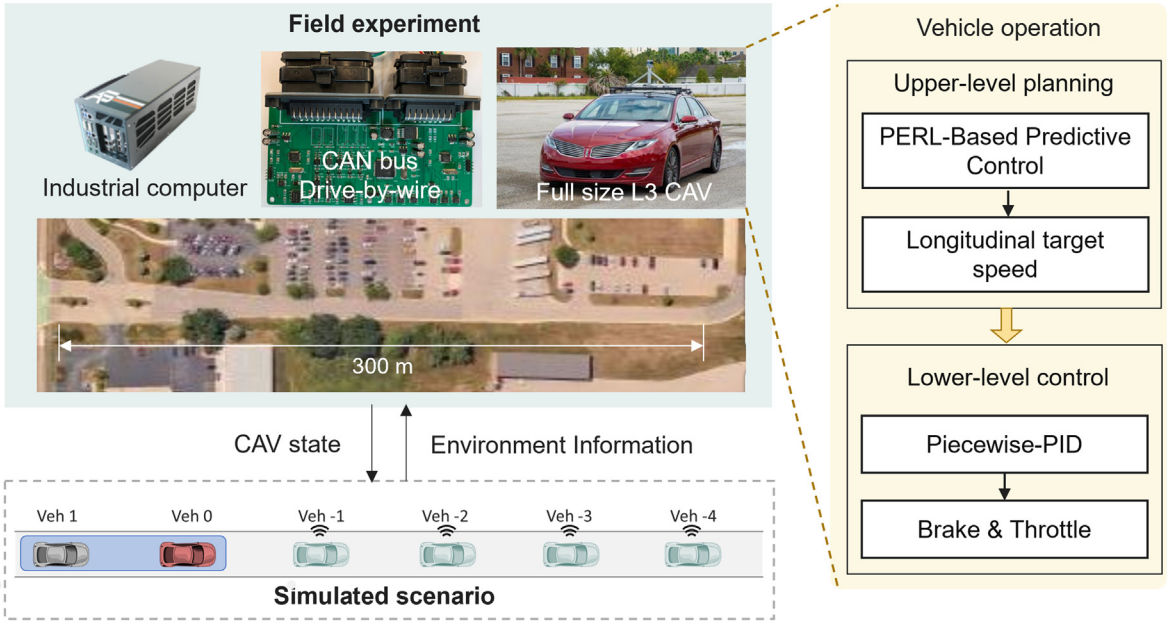

Fig. 4. Vehicle-in-the-loop (ViL) environment.

Table 1
Experimental parameters.

Parameter	Value
Number of vehicles	6
Time interval	0.1 s
Vehicle length, L	4.5 m
Safety distance, S_0	1.5 m
Actuation time lag, τ	0.1
Communication time lag, τ^c	0.2
Acceleration boundary	$[-4\ \mathrm{m/s^2}, 4\ \mathrm{m/s^2}]$
Speed boundary	$[0\ \mathrm{m/s}, 15\ \mathrm{m/s}]$

Fig. 5. Interior view of the experimental vehicle.

consumption. Safety is the foundational premise of the proposed approach, whereas oscillation mitigation and fuel efficiency are the primary objectives of our optimization efforts.

Safety metric: This study chooses a widely employed safety evaluation metric in traffic, the time-to-collision (TTC), to evaluate safety (Kiefer et al., 2005).

$$\mathrm{TTC}_t = \frac{\Delta d_n}{v_n - v_{n-1}} \tag{18}$$

where v_n and v_{n-1} denote the instantaneous velocities of the following and leading vehicles, respectively, and Δd_n represents the spacing between them. A decreased TTC value signifies a greater risk of collision, which is correlated with scenarios where the following vehicle is approaching the leading vehicle at a faster rate relative to their spacing.

Traffic oscillation metric: Oscillation is evaluated at the platoon level via the damping ratio, denoted as d_i, which is used to evaluate the oscillation-dampening performance of a controller over a finite horizon, adapting the concept of acceleration L2 norm string stability typically assessed over an infinite horizon. This ratio is calculated as the square root of the sum of the squared accelerations for vehicle n over T time steps, normalized by the square root of the sum of the squared accelerations for the lead vehicle at time zero; a smaller damping ratio indicates a greater reduction in oscillation magnitude, signifying enhanced controller performance (Ploeg et al., 2014):

$$d_i = \sqrt{\sum_{t=0}^{T} \|a_{nt}\|^2} \Big/ \sqrt{\sum_{t=0}^{T} \|a_{0t}\|^2} \tag{19}$$

Fuel consumption metric: The extensively applied VT-Micro model (Ahn et al., 2002) is chosen for fuel consumption evaluation. This methodology allows for modifications to the running cost function to accommodate alternative methods of estimating instantaneous fuel consumption.

$$\mathrm{MOE}_e\left(v_{n,t}^{\mathrm{sim}}, a_{n,t}^{\mathrm{sim}}\right) = \begin{cases} e^{\sum_{m=0}^{3}\sum_{p=0}^{3}\left(L_{m,p}^{e}\cdot v_{n,t}^{\mathrm{sim}\,m}\cdot a_{n,t}^{\mathrm{sim}\,p}\right)}, a_{n,t}^{\mathrm{sim}} \geq 0 \\ e^{\sum_{m=3}^{3}\sum_{p=0}^{3}\left(M_{m,p}^{e}\cdot v_{n,t}^{\mathrm{sim}\,m}\cdot a_{n,t}^{\mathrm{sim}\,p}\right)}, a_{n,t}^{\mathrm{sim}} < 0 \end{cases} \tag{20}$$

$$e_n^{\mathrm{sim}} = \left(\frac{\sum_{t\in\mathcal{T}} \mathrm{MOE}_e\left(v_{n,t}^{\mathrm{sim}}, a_{n,t}^{\mathrm{sim}}\right) \times 3600}{\sum_{t\in\mathcal{T}} v_{n,t}^{\mathrm{sim}} \times 1000}\right) \div 0.75 \tag{21}$$

where $\mathrm{MOE}_e\left(v_{n,t}^{\mathrm{sim}}, a_{n,t}^{\mathrm{sim}}\right)$ is the instantaneous fuel consumption or emission rate (mg/s). $L_{m,p}^{e}$ and $M_{m,p}^{e}$ represent the model regression coefficients. m and p are power degrees. e_n^{sim} represents the fuel consumption (L/100 km).

4.2. Control performance and data processing

After the experiments concluded, we processed the data collected from the vehicles, primarily focusing on speed and positional information for the analysis phase. The vehicle's speed and position data are sourced

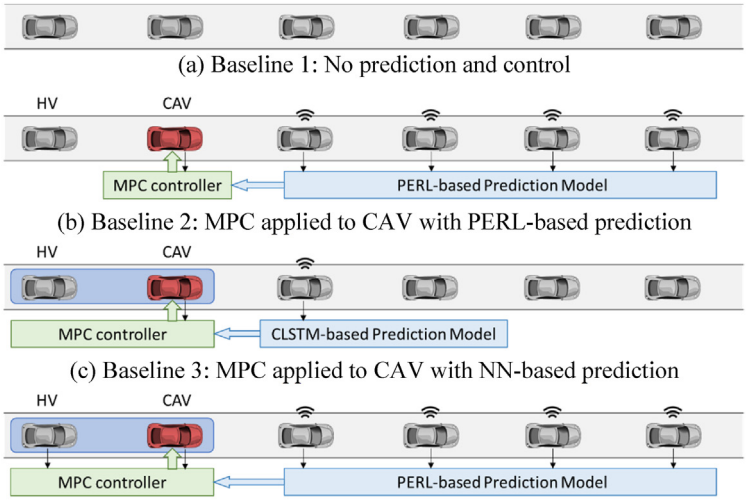

Fig. 6. Researched scenarios. (a) Baseline 1: No prediction and control. (b) Baseline 2: MPC applied to CAV with PERL-based prediction. (c) Baseline 3: MPC applied to CAV with NN-based prediction. (d) Proposed: MPC applied to the mixed platoon of CAV and HV with PERL-based prediction.

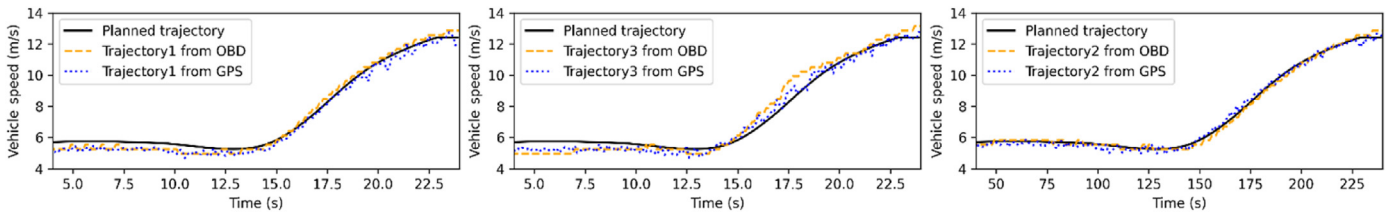

Fig. 7. Expected trajectories with the raw trajectories recorded by OBD and LiDAR across three experiments.

from two systems: vehicle-mounted LiDAR positioning data, which are recorded via the Controller Area Network (CAN) bus. These data are derived from the vehicle's location and tend to be unstable with significant fluctuations, affected by the vehicle's lateral movements. The other source is the on-board diagnostics (OBD), which measures the fuel injector's operation frequency and throttle position. From this, the engine control unit (ECU) can estimate the vehicle's speed. This recorded speed is relatively stable but results in larger errors at lower speeds.

Fig. 7 compares the expected trajectories with the raw trajectories recorded by the OBD and LiDAR across three experiments. Trajectories 1 and 3 represent vehicle movements from south to north, whereas trajectory 2 depicts movement from north to south. The results demonstrate that the speed measurements from both the OBD and LiDAR sources are very similar, with discrepancies primarily due to data noise and the precision limitations of the vehicles.

When the actual vehicle trajectories are compared with the expected trajectories, during the acceleration and cruising phases, the vehicles closely follow the desired speeds. However, performance is slightly less effective during the deceleration phase, resulting in considerable delays. Vehicles tend to decelerate abruptly to match the reduced target speeds only after a delay. To effectively integrate the speed data from both sources, we employ a Kalman filter for smoothing, followed by taking a weighted average of the filtered results.

4.3. Field experiment results

This section first verifies the predictive ability of the proposed PERL-based prediction model for the leading vehicles of CAVs across five selected trips. It then compares the performance of the actual vehicle trajectories following the implementation of the proposed mixed platoon controller with other control strategies over the same five trips.

4.3.1. Prediction results

In Section 4.3, four scenarios are discussed: Baseline1 represents a purely HV environment without predictive capabilities for the preceding vehicle. Both Baseline2 and the proposed method use the same prediction strategy, leveraging information from the four preceding vehicles fed into the PERL model for prediction. Conversely, Baseline3 utilizes data from only the leading vehicle input into a CLSTM model for prediction. Table 2 shows that the PERL-based prediction model has a significantly lower average error than the CLSTM model does, demonstrating the necessity of the PERL model considering multiple preceding vehicles to capture the downstream oscillation characteristics.

Table 2
Preceding vehicle speed prediction RMSE (m/s) of the CLSTM-based and PERL-based prediction models.

Trip	CLSTM-based prediction model (applied in Baseline3)	PERL-based prediction model (applied in Baseline2, proposed)
1	0.157	0.096
2	0.423	0.277
3	0.653	0.408
4	0.461	0.311
5	0.921	0.459
Avg.	0.523	0.310

4.3.2. Safety results

Table 3 compares the minimum TTC during a trip under the proposed method and baseline methods. The TTC remains within a safe range (TTC $>$ 3 s) (Das and Maurya, 2020) under Baseline2, Baseline3, and the proposed method, indicating that all three methods can guarantee safety. Importantly, the goal of this research is not to increase or decrease the TTC but rather to reduce oscillation while ensuring safety. Figs. 8–10 show representative trajectories of acceleration, speed, and position for three scenarios: acceleration, cruising, and deceleration. In all these scenarios, the CAV maintains a stable trajectory and ensures a safe distance from the preceding vehicle.

Notably, in Trip 5, an unsafe scenario occurred: The TTC decreased to 2.29 s because of the leading vehicle's sudden deceleration and the following vehicle's delayed response, as shown in Fig. 10. Under Baseline2, Baseline3, and the proposed method, such unsafe situations are effectively avoided, ensuring that the TTC remains above 2.5 s.

4.3.3. Oscillation results

Table 4 compares the damping ratios of Vehicle 0 and Vehicle 1 relative to Vehicle -1 under both the proposed and baseline methods. In Baseline1, the average damping ratio for Vehicle 0 across five trajectories is 1.062, indicating that in a 100% HV scenario, the speed fluctuations of Vehicle 0 and Vehicle 1 are greater than those of Vehicle -1, leading to the amplification and backward propagation of oscillations. In contrast, the average damping ratios are reduced with the control strategies applied in Baseline2, Baseline3, and the proposed method. Compared with the baseline controllers, the proposed method achieves the lowest average damping ratios for Vehicles 0 and 1 for two main reasons. First, the use of downstream multivehicle information enables the PERL-based prediction model to make more accurate predictions of the preceding vehicle, particularly in capturing oscillation characteristics. This enhances the prediction of oscillation behaviors, facilitating the trajectory planning process of the target CAV. Second, incorporating the behavior of the following vehicle into trajectory planning optimization contributes to stable driving under mixed traffic conditions and helps prevent the propagation of oscillations.

4.3.4. Fuel consumption results

Table 5 compares the fuel consumption throughout the entire trip via the proposed method and baseline methods. In four out of the five scenarios, the proposed method resulted in lower fuel consumption. The improved efficiency can be attributed primarily to the reduced damping ratios achieved under the proposed method, which result in less oscillation and, thus, smoother vehicle dynamics. In Trip 5, an increase in fuel consumption was observed. This anomaly was due to the vehicle needing to decelerate earlier than usual to preemptively address potential safety concerns. The early deceleration led to increased speed variations, resulting in greater fuel usage. This scenario highlights a crucial aspect of vehicle dynamics where safety measures, although necessary, might lead to less efficient fuel usage owing to the required changes in driving patterns.

4.4. Sensitivity analysis

In addition to the field test, this study uses simulation analysis to

Table 3
Minimum TTC(s) results of the three baseline methods and the proposed method.

Trip	Vehicle 0				Vehicle 1			
	Baseline1	Baseline2	Baseline3	Proposed	Baseline1	Baseline2	Baseline3	Proposed
1	13.98	8.96	9.69	9.12	7.96	9.21	8.28	8.65
2	6.75	9.74	8.42	9.76	8.54	11.37	16.23	16.34
3	9.05	72.98	141.71	87.09	11.57	71.58	147.68	88.64
4	17.54	56.31	21.32	31.26	23.43	62.01	21.81	35.33
5	2.29	5.39	4.37	5.42	6.20	7.73	10.83	7.95

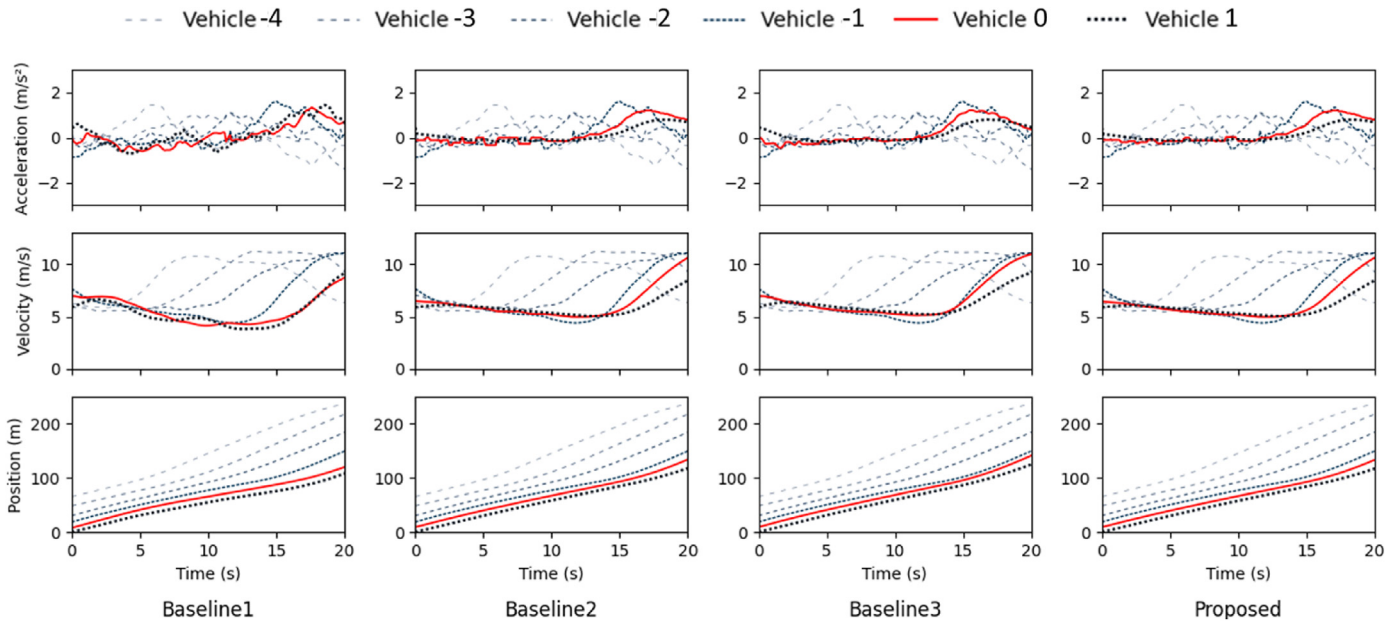

Fig. 8. Vehicle trajectory of Trip 1 (acceleration scenario) under three baseline methods and the proposed method.

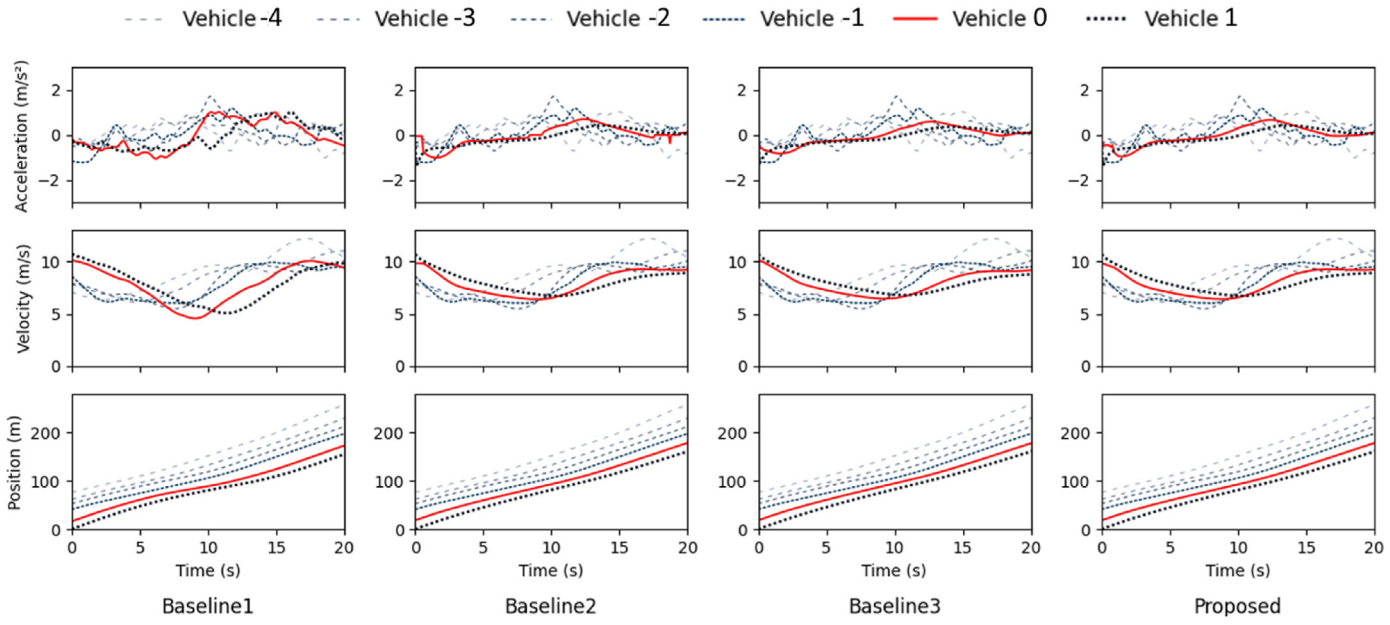

Fig. 9. Vehicle trajectory of Trip 2 (cruising scenario) under three baseline methods and the proposed method.

apply the proposed framework to a larger-scale platoon. We consider a mixed platoon consisting of 30 vehicles, with the lead vehicle's trajectory derived from the NGSIM dataset. This simulation investigates the impact of penetration rates on the framework's effectiveness. The trajectories obtained from the simulation were analyzed, with a focus on oscillation and fuel consumption characteristics. The simulation results indicate that with an increase in the penetration rate of the proposed method-equipped CAVs, the lead vehicle's speed fluctuations dissipate more readily. Fig. 11 compares vehicle trajectories under different CAV penetration rates and reveals that at a 0% penetration rate, shockwaves

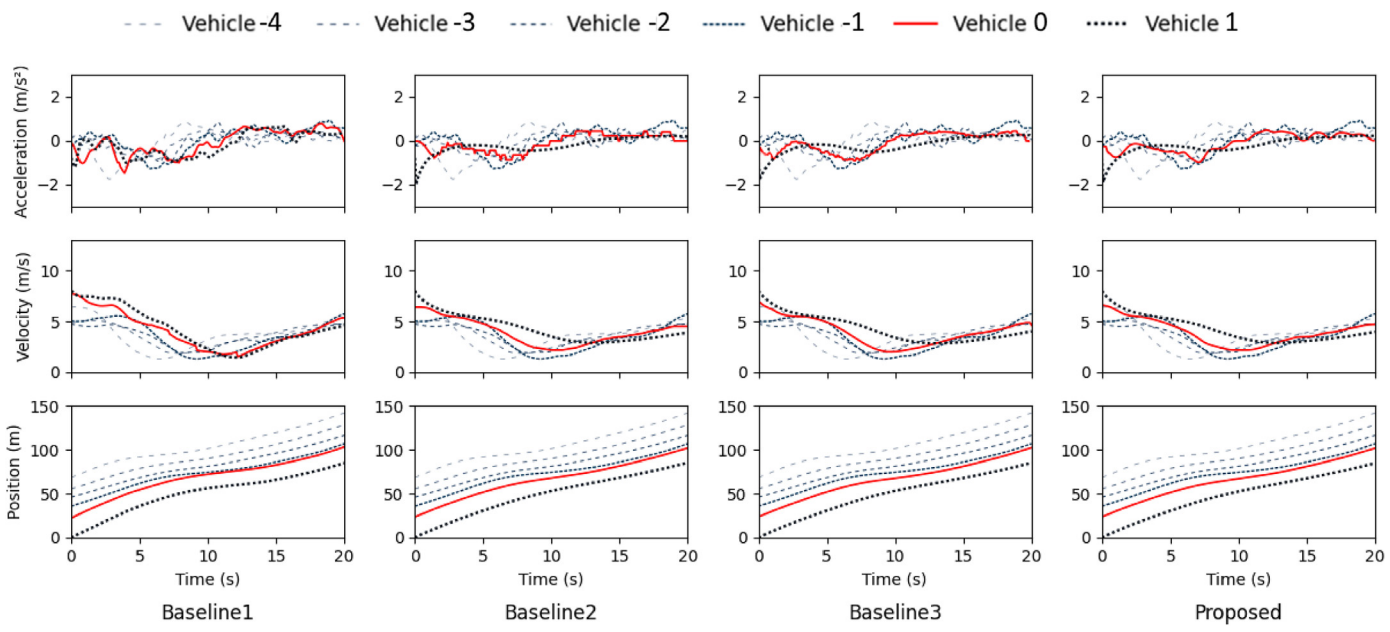

Fig. 10. Vehicle trajectory of Trip 5 (deceleration scenario) under three baseline methods and the proposed method.

Table 4
Damping ratio results of the three baseline methods and the proposed method.

Trip	Vehicle 0				Vehicle 1			
	Baseline1	Baseline2	Baseline3	Proposed	Baseline1	Baseline2	Baseline3	Proposed
1	0.96	0.83	0.83	0.81	1.01	1.02	0.88	0.86
2	1.16	0.81	0.77	0.77	1.27	1.04	0.77	0.79
3	1.23	0.70	0.74	0.71	1.33	0.90	0.73	0.78
4	0.95	0.79	0.69	0.72	1.03	0.88	0.73	0.79
5	1.01	0.87	0.98	0.89	1.09	0.91	1.23	1.04
Avg.	1.062	0.8	0.80	0.78	1.14	0.95	0.87	0.85

Table 5
Fuel consumption (L/100 km) results of the three baseline methods and the proposed method.

Trip	Vehicle 0				Vehicle 1			
	Baseline1	Baseline2	Baseline3	Proposed	Baseline1	Baseline2	Baseline3	Proposed
1	6.779	6.174	6.005	6.025	7.097	7.572	6.310	6.366
2	5.398	5.140	5.130	5.086	5.827	6.557	5.404	4.929
3	7.280	7.127	7.017	7.129	7.860	9.125	6.963	7.927
4	6.664	6.789	6.75	6.387	7.194	7.472	7.083	6.780
5	8.781	8.791	8.926	8.993	9.389	9.172	11.130	10.224
Avg.	6.980	6.804	6.766	6.724	7.473	7.980	7.378	7.285

continuously propagate backward without mitigation. However, as CAV penetration increases, upstream vehicles no longer experience a complete stop, and the magnitude of speed oscillation is reduced. Table 6 contrasts the average damping ratio and fuel consumption across 30 vehicles under varying CAV penetration rates, showing that higher CAV penetration leads to lower average damping ratios—indicating smoother traffic flow and improved fuel efficiency.

5. Conclusions and future research

This study proposes a PERL-based predictive control model for CAVs to mitigate traffic oscillation. The introduced model includes two parts: a PERL-based prediction model and an MPC-based mixed-platoon controller. The prediction model forecasts the future behavior of the preceding vehicle by combining physical shockwave information with neural network techniques. This approach enables precise predictions of speed fluctuations, providing sufficient time for the vehicle or driver to respond effectively. For the PERL-based predictive control model, the dynamics of a CAV and its following vehicles are platooned, resulting in improvements in safety and comfort for the entire platoon. In this study, the proposed mixed-platoon MPC controller is applied to a mixed platoon of CAVs and HVs through ViL and compared with real trajectory data and three benchmark models. The experimental results validate the proposed method in damping traffic oscillation and enhancing the safety and fuel efficiency of the CAV and the following HV in mixed traffic.

For future work, several areas require further investigation. First, the vehicle's lower-level control needs further optimization or integration into the planning process to enhance responsiveness and precision. Second, while the PERL prediction model demonstrated precise predictions via the NGSIM dataset in this research, its predictability in unseen domains or under irrational driving scenarios remains unexplored. Since the model is currently trained on NGSIM data, which primarily include normal driving scenarios, testing its stability and accuracy under other driving conditions (such as weather changes and road friction) is crucial. Moreover, if the behavior of a preceding vehicle exceeds the predictive capabilities of the PERL model, it could indicate irrational driving

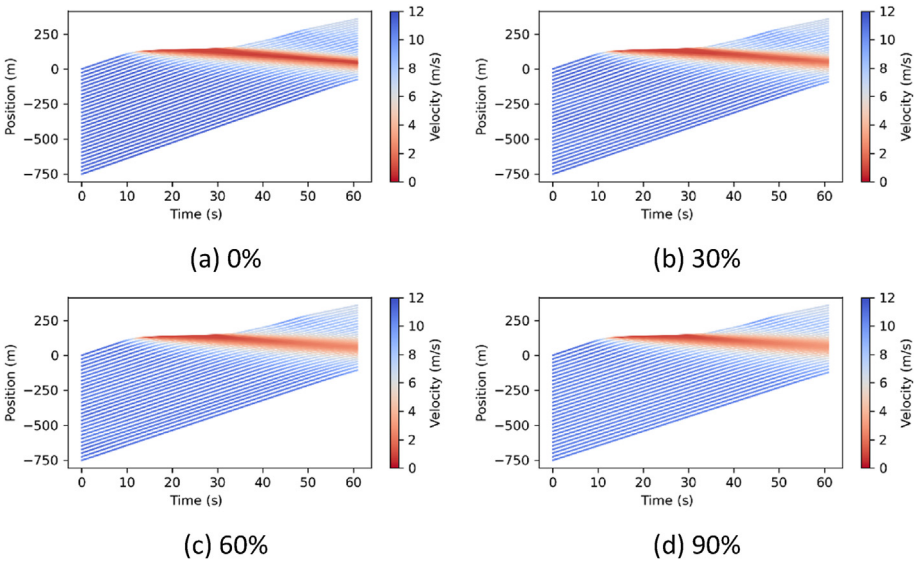

Fig. 11. Trajectories of 30 vehicles via the proposed method under different CAV penetration rates.

Table 6
Average damping ratio and fuel consumption of the platoon of 30 vehicles.

CAV penetration rate (%)	Average damping ratio	Average fuel consumption (L/100 km)
0	0.581	7.882
30	0.498	6.534
60	0.455	5.890
90	0.415	5.414

behavior that might lead to hazardous situations, necessitating proactive maneuvers by following vehicles. Moreover, limited by the experimental conditions of the test track, this study used a ViL setup to examine a specific trajectory. Future research should involve long-duration and long-distance driving in real mixed-flow scenarios to thoroughly test the control effectiveness of the model under actual communication and mechanical delays.

CRediT authorship contribution statement

Keke Long: Writing – original draft, Methodology, Data curation. **Zhaohui Liang:** Validation, Data curation. **Haotian Shi:** Writing – review & editing. **Lei Shi:** Writing – review & editing. **Sikai Chen:** Writing – review & editing. **Xiaopeng Li:** Writing – review & editing, Validation, Supervision, Resources, Project administration, Funding acquisition, Conceptualization.

Replication and data sharing

The data and codes that support the findings of this study are available at https://doi.org/10.26599/ETSD.2024.9190031.

Declaration of competing interest

The authors declare that they have no known competing financial interests or personal relationships that could have appeared to influence the work reported in this paper.

Acknowledgement

This work was supported by the National Science Foundation Cyber-Physical Systems (CPS) program (No. 2343167).

References

Ahn, K., Rakha, H., Trani, A., Van Aerde, M., 2002. Estimating vehicle fuel consumption and emissions based on instantaneous speed and acceleration levels. J. Transport. Eng. 128, 182–190.
Bai, Y., Zhang, Y., Li, X., Hu, J., 2022. Cooperative weaving for connected and automated vehicles to reduce traffic oscillation. Transp. A Transp. Sci. 18, 125–143.
Chen, D., Laval, J., Zheng, Z., Ahn, S., 2012. A behavioral car-following model that captures traffic oscillations. Transp. Res. Part B Methodol. 46, 744–761.
Chen, N., Wang, M., Alkim, T., van Arem, B., 2018. A robust longitudinal control strategy of platoons under model uncertainties and time delays. J. Adv. Transport. 2018, 9852721.
Das, S., Maurya, A.K., 2020. Defining time-to-collision thresholds by the type of lead vehicle in non-lane-based traffic environments. IEEE Trans. Intell. Transport. Syst. 21, 4972–4982.
Durrani, U., Lee, C., Maoh, H., 2016. Calibrating the Wiedemann's vehicle-following model using mixed vehicle-pair interactions. Transport. Res. C Emerg. Technol. 67, 227–242.
Fang, S., Yang, L., Zhao, X., Wang, W., Xu, Z., Wu, G., et al., 2024. A dynamic transformation car-following model for the prediction of the traffic flow oscillation. IEEE Intell. Transport. Syst. Mag. 16, 174–198.
Gao, Z., Wu, Z., Hao, W., Long, K., Byon, Y.J., Long, K., 2022. Optimal trajectory planning of connected and automated vehicles at on-ramp merging area. IEEE Trans. Intell. Transport. Syst. 23, 12675–12687.
Ghiasi, A., Li, X., Ma, J., 2019. A mixed traffic speed harmonization model with connected autonomous vehicles. Transport. Res. C Emerg. Technol. 104, 210–233.
He, Y., Liu, Y., Yang, L., Qu, X., 2024. Deep adaptive control: deep reinforcement learning-based adaptive vehicle trajectory control algorithms for different risk levels. IEEE Trans. Intell. Veh. 9, 1654–1666.
Hu, J., Zhang, Z., Xiong, L., Wang, H., Wu, G., 2021. Cut through traffic to catch green light: Eco approach with overtaking capability. Transport. Res. C Emerg. Technol. 123, 102927.
Karniadakis, G.E., Kevrekidis, I.G., Lu, L., Perdikaris, P., Wang, S., Yang, L., 2021. Physics-informed machine learning. Nat. Rev. Phys. 3, 422–440.
Kiefer, R.J., LeBlanc, D.J., Flannagan, C.A., 2005. Developing an inverse time-to-collision crash alert timing approach based on drivers' last-second braking and steering judgments. Accid. Anal. Prev. 37, 295–303.
Larsson, J., Keskin, M.F., Peng, B., Kulcsár, B., Wymeersch, H., 2021. Pro-social control of connected automated vehicles in mixed-autonomy multi-lane highway traffic. Commun. Transp. Res. 1, 100019.
Li, J., Xie, N., Zhang, K., Guo, F., Hu, S., Chen, X., 2022. Network-scale traffic prediction via knowledge transfer and regional MFD analysis. Transport. Res. C Emerg. Technol. 141, 103719.

Li, X., Cui, J., An, S., Parsafard, M., 2014. Stop-and-go traffic analysis: theoretical properties, environmental impacts and oscillation mitigation. Transp. Res. Part B Methodol. 70, 319–339.
Li, X., Peng, F., Ouyang, Y., 2010. Measurement and estimation of traffic oscillation properties. Transp. Res. Part B Methodol. 44, 1–14.
Li, X., Wang, X., Ouyang, Y., 2012. Prediction and field validation of traffic oscillation propagation under nonlinear car-following laws. Transp. Res. Part B Methodol. 46, 409–423.
Li, Y., Li, Z., Wang, H., Wang, W., Xing, L., 2017. Evaluating the safety impact of adaptive cruise control in traffic oscillations on freeways. Accid. Anal. Prev. 104, 137–145.
Li, Z., Xu, C., Guo, Y., Liu, P., Pu, Z., 2021. Reinforcement learning-based variable speed limits control to reduce crash risks near traffic oscillations on freeways. IEEE Intell. Transport. Syst. Mag. 13, 64–70.
Lighthill, M.J., Whitham, G.B., 1997. On kinematic waves II. A theory of traffic flow on long crowded roads. Proc. Roy. Soc. Lond. Math. Phys. Sci. 229, 317–345.
Long, K., Sheng, Z., Shi, H., Li, X., Chen, S., Ahn, S., 2024a. A physics enhanced residual learning (PERL) framework for vehicle trajectory prediction. https://doi.org/10.48550/arXiv.2309.15284.
Long, K., Shi, H., Chen, Z., Liang, Z., Li, X., de Souza, F., 2024b. Bi-scale car-following model calibration based on corridor-level trajectory. Transport. Res. Part E Logist. Transp. Rev. 186, 103497.
Mo, Z., Shi, R., Di, X., 2021. A physics-informed deep learning paradigm for car-following models. Transport. Res. C Emerg. Technol. 130, 103240.
Mohammadian, S., Zheng, Z., Haque, M.M., Bhaskar, A., 2023. Continuum modeling of freeway traffic flows: state-of-the-art, challenges and future directions in the era of connected and automated vehicles. Commun. Transp. Res. 3, 100107.
NGSIM, 2007. US Department of Transportation, NGSIM-Next generation simulation. https://ops.fhwa.dot.gov/trafficanalysistools/ngsim.htm.
Ploeg, J., van de Wouw, N., Nijmeijer, H., 2014. Lp string stability of cascaded systems: application to vehicle platooning. IEEE Trans. Control Syst. Technol. 22, 786–793.
Punzo, V., Montanino, M., 2020. A two-level probabilistic approach for validation of stochastic traffic simulations: impact of drivers' heterogeneity models. Transport. Res. C Emerg. Technol. 121, 102843.
Qu, X., Yu, Y., Zhou, M., Lin, C.T., Wang, X., 2020. Jointly dampening traffic oscillations and improving energy consumption with electric, connected and automated vehicles: a reinforcement learning based approach. Appl. Energy 257, 114030.
She, R., Ouyang, Y., 2024. Hybrid truck–drone delivery under aerial traffic congestion. Transp. Res. Part B Methodol. 185, 102970.
Stern, R.E., Chen, Y., Churchill, M., Wu, F., Delle Monache, M.L., Piccoli, B., et al., 2019. Quantifying air quality benefits resulting from few autonomous vehicles stabilizing traffic. Transport. Res. Transport Environ. 67, 351–365.
Wang, J., Zheng, Y., Dong, J., Chen, C., Cai, M., Li, K., et al., 2024. Implementation and experimental validation of data-driven predictive control for dissipating stop-and-go waves in mixed traffic. IEEE Internet Things J. 11, 4570–4585.
Wang, S., Shang, M., Levin, M.W., Stern, R., 2023. A general approach to smoothing nonlinear mixed traffic via control of autonomous vehicles. Transport. Res. C Emerg. Technol. 146, 103967.
Xu, Z., Wang, M., Zhang, F., Jin, S., Zhang, J., Zhao, X., 2017. PaTAVTT: a hardware-in-the-loop scaled platform for testing autonomous vehicle trajectory tracking. J. Adv. Transport. 2017, 9203251.
Yao, H., Li, Q., Li, X., 2022. Trajectory prediction dimensionality reduction for low-cost connected automated vehicle systems. Transport. Res. Transport Environ. 111, 103439.
Yao, H., Li, Q., Li, X., 2020. A study of relationships in traffic oscillation features based on field experiments. Transport. Res. Part A Policy Pract. 141, 339–355.
Yao, H., Li, X., Yang, X., 2023. Physics-aware learning-based vehicle trajectory prediction of congested traffic in a connected vehicle environment. IEEE Trans. Veh. Technol. 72, 102–112.
Zheng, S.T., Jiang, R., Tian, J., Li, X., Treiber, M., Li, Z.H., et al., 2022. Empirical and experimental study on the growth pattern of traffic oscillations upstream of fixed bottleneck and model test. Transport. Res. C Emerg. Technol. 140, 103729.
Zhou, M., Qu, X., Li, X., 2017. A recurrent neural network based microscopic car following model to predict traffic oscillation. Transport. Res. C Emerg. Technol. 84, 245–264.

Keke Long is a Ph.D. candidate in the Department of Civil and Environmental Engineering at the University of Wisconsin–Madison (UW–Madison), USA. She obtained the B.S. degree in traffic engineering from Changan University, Xi'an, China in 2018 and the M.S. degree in traffic engineering from Tongji University, Shanghai, China in 2021. Her main research interests are the artificial intelegence application in perception and autonomous vehicle control.

Zhaohui Liang is a Ph.D. candidate in the Department of Civil and Environmental Engineering at UW–Madison. He obtained the B.S. degree from Harbin Institute of Technology, Weihai, China in 2019. His main research interests are Eco-driving algorithms and connected autonomous vehicles testing.

Haotian Shi is a Research Associate at UW-Madison. He received the Ph.D. degree in civil & environmental engineering from UW-Madison in 2023. He obtained three M.S. degrees in computer science (UW–Madison, 2022), civil and environmental engineering (UW–Madison, 2020), and power and machinery engineering (Tianjin University, 2020). He also obtained double B.S. degrees in computer science (2017) and energy and power engineering (2017) from Tianjin University. His research directions focus on the prediction & control of Connected Automated Vehicles (CAVs), intelligent transportation systems, traffic crash data analysis, and deep reinforcement learning.

Lei Shi is currently pursuing the Ph.D. degree in the Department of Civil and Environmental Engineering at UW–Madison. He received the B.E. degree in energy and power engineering from Shandong University, China, in 2020 and the M.S.E. degree in robotics engineering from Johns Hopkins University, USA, in 2022. His primary research interests include robotics and autonomous vehicles.

Sikai Chen is an Assistant Professor at the Department of Civil and Environmental Engineering and the Department of Mechanical Engineering (courtesy), UW–Madison. He received the Ph.D. degree in civil engineering with a focus on computational science & engineering from Purdue University in 2019. His research focuses on three major themes: human users, AI, and transportation. He aims to innovate and develop safe, efficient, sustainable, and human-centered transportation systems by cutting-edge methods and technologies. The focus is on incorporating human behaviors, interactive autonomy, digital infrastructure, and intelligent control frameworks. In addition, he is a member of two ASCE national committees: Connected & Autonomous Vehicle Impacts, and Economics & Finance; IEEE Emerging Transportation Technology Testing Technical Committee; and TRB Standing Committee on Statistical Methods (AED60).

Xiaopeng Li is currently a Professor in the Department of Civil and Environmental Engineering and an affiliate in the Department of Electrical and Computer Engineering at UW–Madison. He served as the Director of National Institute for Congestion Reduction (NICR) before. He is a recipient of a National Science Foundation (NSF) CAREER award. He has published over 110 peer-reviewed journal papers. He has served as the PI or a co-PI for a number of federal, state, and industry grants, with a total budget of around $30 million. His major research interests include automation, connectivity, and sensing in transportation and related systems. He received the B.S. degree (2006) in civil engineering with a minor in computer engineering from Tsinghua University, China, the M.S. degree (2007), and the Ph.D. (2011) degree in civil engineering along with the M.S. degree (2010) in applied mathematics from the University of Illinois at Urban-Champaign, USA.